PLASTIC DEFORMATION OF α TITANIUM ALLOYS SHEETS

Authors: Dr. Eng. Silvia Gaiani (*Akrapovič d.d., Technical Director)*
Sebastijan Jurendić B. Sc. (*Akrapovič d.d., CAE Simulation)*
Prof. Paolo Veronesi *(Materials Engineering Dept. – Modena University)*

ABSTRACT

Titanium alloys used for exhaust system fabrication are currently all α alloys, which use small quantities of different alloying elements, such as aluminum, copper, niobium, silicon and iron. These advanced alloys show excellent properties for their target application (high strength, resistance to high-temperature oxidizing environments, weldability); however, their use for producing parts with complicated shapes is still limited, due to problems associated with poor formability and consequently high manufacturing costs.
In order to predict formability and anisotropic behavior of this type of α titanium alloys, a large variety of experimental tests have been performed, with the aim to collect a complete set of data, which can be used to build a dedicated anisotropic mathematical model that precisely describes the behavior of the material during plastic deformation.
For predicting titanium α alloys deformation, in the present study the Barlat's anisotropic yield function has been chosen and used in a series of FAE analysis.
The paper describes the experimental procedure used to collect a data set necessary for FEA simulation and the procedure used to validate the numerical model. A comparison between simulation and real deformation processes is presented and discussed.

1.0 INTRODUCTION

With the ever widening use of titanium alloys in commercial applications, classical manufacturing technologies are being applied to the production of components from these materials. This can pose a problem under mass production conditions, since the mechanical properties of these materials can be quite different from those of traditional engineering materials.
One example is deep drawing of heat resistant titanium alloy sheet. In some applications, such as high-end automotive exhausts, the exceptional mechanical, thermal and corrosion-resistant properties of titanium outweigh the high cost of the raw material and the complexities of production. However, to successfully implement deep drawing in an industrial environment, some deeper understanding of the mechanisms of plasticity, which occur in these materials, is needed.
The properties that make titanium sheet problematic for deep drawing are poor strain hardening and high anisotropy. While hardening properties in the rolling direction are somewhat acceptable, they deteriorate significantly toward the transverse direction. This is a consequence of the crystal structure and to some extent the rolling process and cannot be avoided.
Advanced numerical simulations provide for a deeper insight into the mechanics of sheet metal forming, that would otherwise be impossible, and to efficiently optimize the forming processes without the need for extensive trials.

2.0 CRISTALLOGRAPHIC PROPERTIES

Titanium alloys used for high temperature applications are all α alloys with a hexagonal close packed crystal structure. Small quantities of different alloying elements, such as aluminum, copper, niobium, silicon and iron are added to significantly increase the oxidation resistance and mechanical properties in comparison to commercially pure titanium, especially Grade 2. They do not however significantly affect the crystal structure. These advanced alloys show excellent properties for their target application (high strength, elevated thermal properties, weldability); however, their use for producing parts with complicated shapes is still limited because of problems associated with poor formability and consequently high manufacturing costs. α Titanium alloys have intrinsically anisotropic characteristics that are mainly related

to two fundamental aspects of their microstructure:

- Asymmetric geometry of the HCP crystallographic structure and its slipping planes
- Preferred crystallographic orientation after cold rolling (texturing)

In HCP metals, the deformation modes and texturing are primarily determined by c/a ratio. For titanium, the hexagonal unit cell of the α phase has values of the lattice parameters a=0.295 nm and c=0.468 nm. The resulting c/a ratio for pure α titanium is 1.587, rather smaller than the value 1.633 for ideal close packing of spheres.

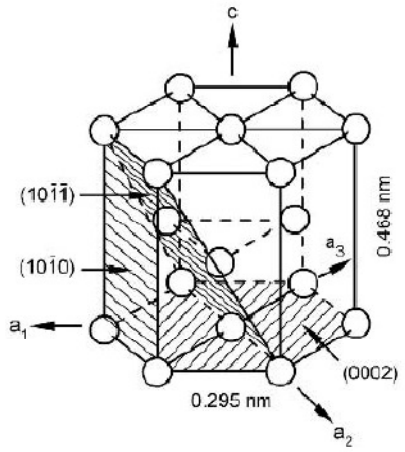

Pic. 1 – HCP unit cell with slip planes [1]

Due to the c/a ratio being smaller than ideal in the HCP structure of α Ti, only 4 independent slip systems for dislocation movement are available. However, according to the Von Mises principle, to obtain homogeneous plastic deformation at least five independent slip systems are required [2]. This means that in order to have plastic deformation, a system with a non-basal Burgers vector has to be activated. The need to activate two different types of dislocations simultaneously is strictly related to the direction of loading. For all these reasons, plastic deformation in α titanium alloys is strongly dependent on the activation of twinning deformation modes in addition to conventional slip by dislocations. To be more precise, these twinning modes are probably the most important for the deformation behavior of the considered α titanium alloys.

The c/a ratio plays a vital role also in texturing phenomena. In fact, it is well known that during cold rolling, α titanium alloys show a considerable tendency toward a preferred crystallographic orientation. The orientation of the lattice is related to many factors like the c/a ratio, rolling conditions, annealing temperature, etc. Most HCP alloys show a nearly basal texture (i.e. c-axis aligned normal to the plane of the sheet); for α titanium alloys obtained with standard production processes the basal planes are inclined approximately ±30° in the transverse direction [3]. However, certain alloying agents, cross rolling, heat treatment temperature also play an important role in determining the final texturing direction of the material.

3.0 SHEET FORMABILITY OF ANISOTROPIC MATERIALS

Different dislocation slip systems and the effects of texture have a considerable influence on strain distribution and plastic flow of the material during sheet forming operations. Particularly interesting from an industrial point of view is the deep drawing process, where a punch and a die are used to deform a flat blank into a three dimensional flanged part. In fact, in order to obtain extensive deformation during drawing operations it is necessary that the metal flow in the flange region can occur easily without the buildup of high stresses which can cause fracture at the die radius.

Texturing in metal sheet can have two types of influences on deep drawability [4]:

- If plastic flow properties differ depending on a direction in the metal sheet plane, the flow of material will not be constant around the periphery of the drawn cup (earing); this phenomenon is related to planar anisotropy
- When differential strengthening between in-plane (flange) and the through thickness (punch) is present, the plastic flow of the material is directly dependent on the normal anisotropy

Both normal and planar anisotropy are extremely important for predicting drawability, because they depend on plastic flow processes which take place in different areas of the metal. These two parameters can be easily obtained by measuring the plastic strain ratio (Lankford value), defined as the ratio between true strains in the width and thickness directions [5]. Thus:

$$R = \frac{\varepsilon_w}{\varepsilon_t}$$

The R-value can be easily obtained by performing a standard tensile test and measuring elongation

of the specimen and its width reduction with a bidirectional strain gauge. Considering that the volume of a solid during plastic deformation is invariable, this parameter can be expressed as follows:

$$R = \frac{-\varepsilon_w}{\varepsilon_l + \varepsilon_w}$$

Assuming that the rolling direction has an orientation of 0°, the transverse direction an orientation of 90° and the diagonal direction an orientation of 45°, normal and planar anisotropy are defined as follows:

$$\overline{R} = \frac{(R_{00} + 2R_{45} + R_{90})}{4} \text{ (normal anisotropy);}$$

$$\Delta R = \frac{(R_{00} - 2R_{45} + R_{90})}{2} \text{ (planar anisotropy)}$$

3.1 Experimental data collection

In order to compare the plastic behavior of two α titanium alloys produced by the Japanese manufacturer KOBE Steel, 1.2ASN and 1.5AL, a series of standard tensile tests has been carried out along three different directions: rolling (0°), transverse (90°) and diagonal (45°).
A bidirectional gauge was used for strain determination. Using this type of instrument, the elongation of the specimens in longitudinal direction (ε_l) and the width reduction (ε_w) can be recorded, thus all the parameters related to the anisotropy of the material can be measured.

3.1.1 Tensile testing results

The tensile tests have been carried out in accordance with the EN 10002/1 standard with the extensimeter gauges at 80 mm. 9 specimens have been tested in every direction for each material. The average values of all the tests are shown in table n°1:

Mat.	Dir.	Rp (MPa)	Rm (MPa)	A_{gt} (%)	A_{80} (%)	E (GPa)
1.2ASN	0°	323	457	18,4	32,1	107
	90°	394	437	9,0	34,5	119
	45°	355	417	15,7	35,9	109
1.5 AL	0°	312	442	13,3	30,5	105
	90°	367	414	7,1	32,1	115
	45°	334	398	8,8	33,8	112

Tab. 1 – Tensile test results

3.1.2 Lankford coefficients

The evaluation of plastic strain ratio and anisotropy coefficients has been carried out in accordance with the ASTM E517 and ISO 10113 standards. The average values of all the tests are shown in table n°2:

Mat.	$R_{0°}$	$R_{90°}$	$R_{45°}$	R	ΔR
1.2 ASN	1,6	4,3	2,7	2,825	0,25
1.5 AL	2,8	7,4	4,3	5,600	0,80

Tab. 2 – Lankford coefficients

3.1.3 Strain hardening coefficients

The evaluation of strain hardening exponent and coefficient has been carried out in accordance with the ASTM E646 and ISO 10275 standards. The average values of all the tests are shown in table n°3:

Mat.	$n_{0°}$	$K_{0°}$ (MPa)	$n_{90°}$	$K_{90°}$ (MPa)	$n_{45°}$	$K_{45°}$ (MPa)
1.2ASN	0,154	710	0,086	590	0,112	596
1.5 AL	0,137	668	0,087	563	0,108	569

Tab. 3 – Strain hardening coefficients

4.0 MODELLING OF THE PLASTIC RESPONSE USING THE BARLAT COSTITUTIVE EQUATION

The Barlat [1989] plane stress anisotropic yield criterion, developed by Barlat and Lian [4], was chosen for the simulation because it can directly accept all data derived from the in-house uniaxial tensile test and has an adaptable yield locus. It was primarily designed for FCC and BCC materials so it lacks the capacity for emulating advanced phenomena associated with HCP materials, however it should give acceptable results for simple, predominantly tensile load paths, where asymmetries between yielding in tension and compression can be neglected [6].

4.1 Yield criterion

The anisotropic plane stress yield criterion is defined as:

$$\Phi = a|K_1 + K_2|^m + a|K_1 - K_2|^m + c|2K_2|^m = 2\sigma_Y{}^m$$

Where K_1 and K_2 are defined as:

$$K_1 = \frac{\sigma_x + h\sigma_y}{2};\ K_2 = \sqrt{\left(\frac{\sigma_x - h\sigma_y}{2}\right)^2 + p^2\tau_{xy}{}^2}$$

a, *c*, *h*, *p*, *m* are material parameters defined as:

$$a = 2 - 2\sqrt{\frac{R_{00}}{1+R_{00}} \cdot \frac{R_{90}}{1+R_{90}}} \quad ; \quad c = 2 - a \quad ;$$

$$h = \sqrt{\frac{R_{00}}{1+R_{00}} \cdot \frac{1+R_{90}}{R_{90}}}$$

According to the authors of the yield criterion the width to thickness strain ratio *R* for an arbitrary angle from the rolling direction can be determined by:

$$R_{\phi} = \frac{2m\sigma_Y{}^m}{\left(\frac{\partial\Phi}{\partial\sigma_x} + \frac{\partial\Phi}{\partial\sigma_y}\right)\sigma_{\phi}} - 1$$

And the parameter *p* is calculated iteratively from the above expression to fit the data for the uniaxial tensile test in the diagonal (45°) direction.
Picture n°2 shows the Barlat yield locus compared to the Von Mises criterion at the same yield stress.

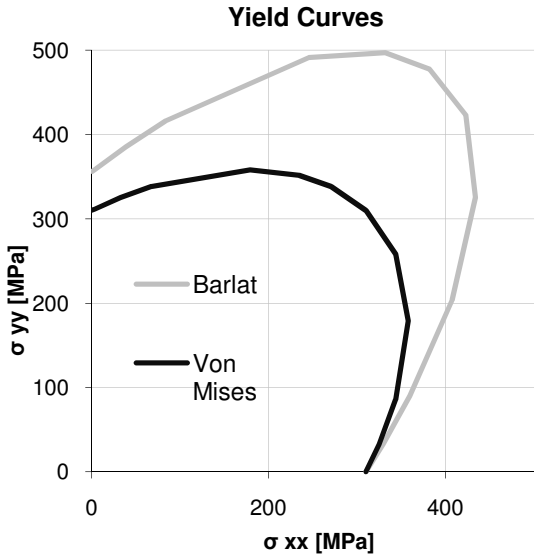

Pic. 2 – Yield locus for Barlat and Von Mises

4.2 Input data

The necessary input data for the yield criterion are:

- Lankford coefficients in three directions: R_{00}, R_{45}, R_{90}, which are derived directly from the tensile test with the width to thickness strain ratio measurement. They do not vary significantly with strain, so the average value of all the measurements in a given direction is used.
- Yield stress as a function of equivalent plastic strain $\sigma_Y\left(\bar{\varepsilon}_p\right)$ in the rolling direction, which can be expressed by two different methods: using a mathematical function (i.e. the Hollomon equation [7]) or using an experimental curve derived directly from the tensile test.
- Flow potential exponent *m*, a parameter which defines the shape of the yield locus. The authors of the model specify recommended values for face centered cubic and body centered cubic materials, however little reference to HCP materials is found in literature, and thus a separate evaluation has been carried out.

4.3 Yield – Stress curve determination

Initially the Hollomon equation $\sigma = K \cdot \varepsilon^n$ was used as the yield stress function, however the fit at higher strains is poor. In contrast to steel, titanium exhibits substantial additional elongation past R_m, with a fairly gradual onset of localization, which is in line with the properties expected from its crystal structure. This property becomes even more pronounced in the diagonal and transverse direction where the peak force occurs at very low strains yet the material still achieves a moderate strain at fracture. The assumption follows that quite some useful deformation occurs after the onset of localized thinning in metal forming applications. This property cannot be reasonably captured by any of the traditional hardening laws, and since the simulation software enables the use of an arbitrary curve for the material hardening property, there is no need to develop a new functional approximation.
To accurately describe the plastic response in our specific case, a true stress-true strain curve is used. Up to the onset of localization the data from the tensile test is used as the stresses and strains can be accurately determined under homogeneous stress conditions. Past R_m a non-trivial triaxial stress state develops in the necking region and the remainder of the curve is identified via an inverse procedure, where numerical simulations of the tensile test are used to iteratively modify the load curve until the calculated response matches the data from the tensile test [8].

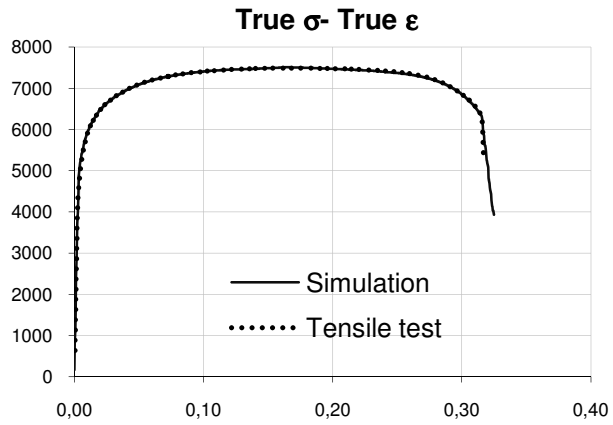

Pic. 3 – Tensile test simulation for 1.2 ASN

A fit within the scatter between samples of the same batch can be achieved without difficulties; however, since the deviation of material properties on a single coil of sheet is usually substantial, a perfect fit is not necessary. Picture n°3 shows the results of such an inverse procedure, the fit between the measured and calculated σ-ε curves is practically perfect through the range. The stress-strain curve from the simulation continues past the breaking point because there is no damage model implemented, it is up to the user to identify whether or not the maximum strain has been surpassed. This is usually accompanied by severe unrealistic deformation or local instabilities of the model.

The final load curve for the material is shown in picture n°4 along with the measured true σ – true ε curve and the functional approximation using the Hollomon power law. Compared to the Hollomon approximation it is somewhat steeper to support the extensive post-R_m deformation. Also note how far past the global strain at breaking the curve extends, this offers some insight into the materials behavior in the necking region after the onset of localized deformation.

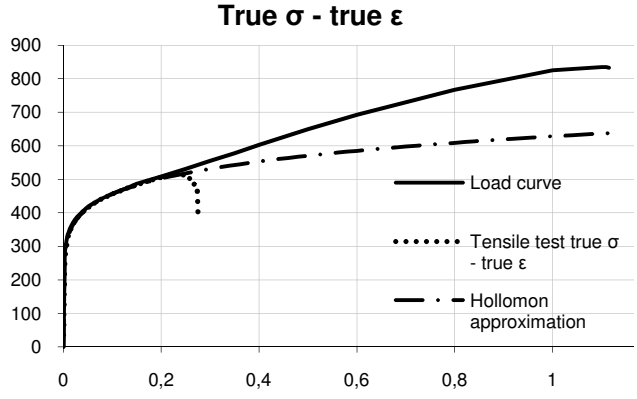

Pic. 4 – The inversely identified load curve

4.4 Determination of m parameter

The *m* parameter controls the shape of the yield locus, thus a biaxial test should be used to evaluate the proper value. The Erichsen cupping test was chosen because of its simple application in an industrial environment on a standard testing machine. The equal biaxial tension induced in the specimen is suitable for evaluation of phenomena associated with anisotropy, as no direction is favored. Similarly to the yield curve identification, numerical simulations were run for a range of *m* parameters and the results were compared to the experimental data.

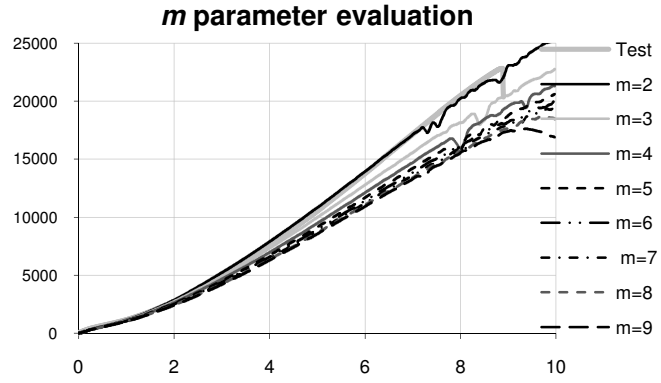

Pic. 5 – Evaluation of m parameter using Erichsen test

The results show best compliance with the experimental data for *m=2*. This is in accordance with some research on the subject [9] where titanium was identified as having a quadratic yield locus. The fit of the force-deflection curve is quite satisfactory; however a perfect fit cannot be expected since several values, other than the material properties, influence the result. Friction parameters, numerical model design and meshing, and the simulation parameters all add an error that is difficult to assess. Similar to the tensile test simulation, the force-deflection curve continues past the breaking point for the same reason.

5.0 LIMITS 0F DEFORMATION: FLD DIAGRAM

As shown in section 4.4, the force–displacement characteristics of the Erichsen test are matched quite well by the simulation, leading to the conclusion that the constitutive model can accurately recreate the stress-strain state in the material during deformation. Also outlined is the fact that the simulation itself cannot explicitly predict material breaking due to the lack of an

explicit damage model. Discontinuities in the form of unrealistic deformation do occur, however they always succeed actual material breaking if the model is properly meshed.
While valuable information for forming process calibration can be obtained nonetheless, the primary goal of the simulation is to determine the feasibility of the forming process, thus some means of gauging the achievable deformation needs to be implemented. For this reason the well known forming limit diagram is used. The strains can easily be obtained from the simulation and compared to the experimental forming limit curves to determine whether or not material defects should be expected.
In order to determine the upper limit of formability for the two considered titanium alloys, a series of compression tests using a hemi-spherical punch has been carried out at the Erlangen University using the Aramis optical 3D forming analysis system for strain measurement. This system recognizes a stochastical pattern, spray-painted on the specimen surface, using two cameras recording the deformation process in real time (picture n°6).

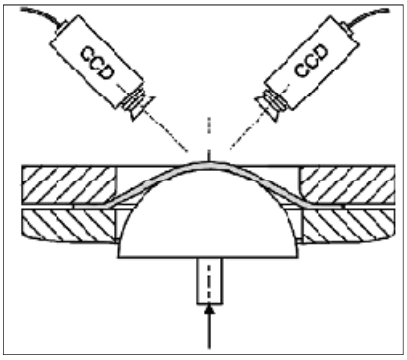

Pic. 6 – Aramis equipment displacement during the test

In our specific case the well known Nakajima method for determining the forming limit curve has been used. With this type of test the minor strain is varied using specimens with different elliptical aspect ratios, as shown in picture n°7.

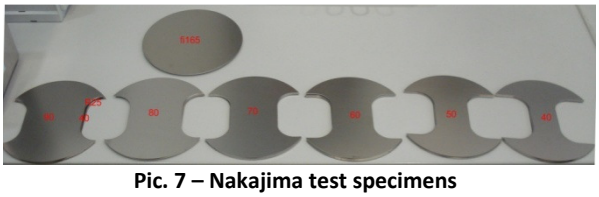

Pic. 7 – Nakajima test specimens

The tests have been performed using three specimens of seven different geometries, extracted along the rolling and transverse direction; for each alloy a total of 42 tests were performed. The forming limit diagrams obtained for 1.2 ASN is showed below.

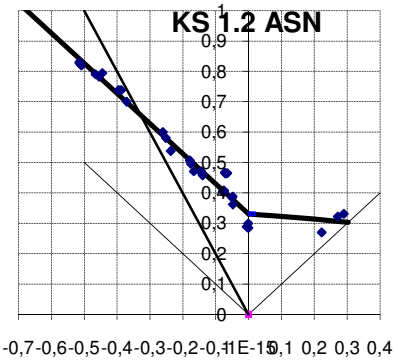

Pic. 8 – FLD diagram for 1.2 ASN

6.0 EXAMPLE OF SIMULATION

To verify the method a numerical simulation of a deep drawing process has been carried out. The part chosen is an end-cap on an exhaust muffler that is problematic from a production standpoint, i.e. it can be drawn from the 1.5AL material, but not from 1.2ASN, despite the Lankford parameters showing less anisotropy for the second material which normally means better formability.
The software used for the simulation was LS-Dyna explicit solver along with LS-PrePost. The solution was time and mass-scaled to shorten calculation time and adaptive re-meshing of the blank was implemented. The Barlat [1989] material model is already implemented in the software as LS-Dyna material model number 36. It also has the benefit of calculating the material parameters internally from the R-values, which are input directly.

6.1 Numerical model

Shell elements were used for the entire model, the tools being considered rigid. Orientation of the material on the blank was with the rolling direction along the length of the rosette, as tests indicated the best results in this alignment. The punch is prescribed a constant velocity to a displacement of 90 mm and is than retracted for spring back analysis, the blank holder is loaded with a constant force of 98,1 kN (10 metric tons) and frictional contacts were defined for tool-blank interactions.

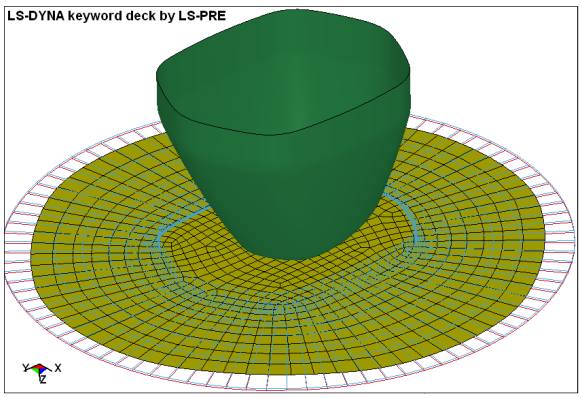

Pic. 9 – Numerical model of the drawing process

6.2 Comparison between numerical and experimental results

The results of the simulation correlate well to the deep drawing tests. The Q9 endcap could be drawn from the 1.5 AL material and not from 1.2 ASN. Similarly, the simulations exhibit various indicators of material failure for 1.2 ASN, while no problems are encountered while using the material parameters for 1.5 AL.

The following aspects of the simulation were evaluated when processing the results:

- Stress distribution and maximum achievable load during deformation
- Mayor-minor strains plotted on the FLD diagram
- Thickness distribution

6.2.1 Stress distribution

The simulation using 1.2 ASN alloy shows strong stress localization around the leading edge of the punch, at around 30 mm of displacement there is excessive stretching of the blank that the mesh cannot accommodate, indicating material failure.

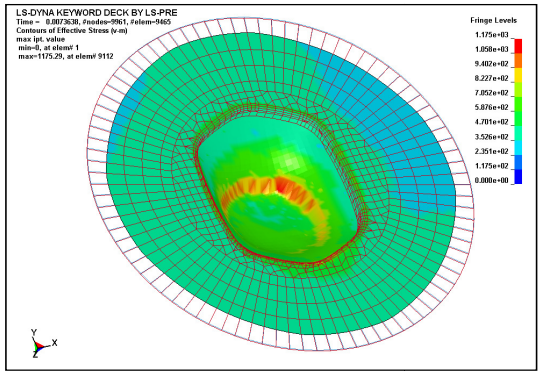

Pic. 10 – Von Mises effective stress for 1.2 ASN

This result is also confirmed with the force-displacement plot, where the degradation of the blank at around 30 mm displacement is clearly visible.

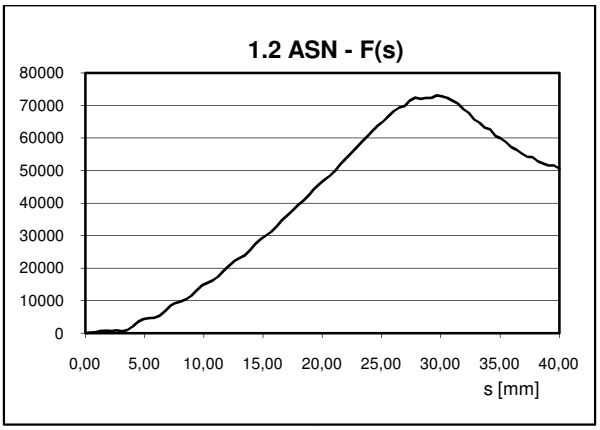

Pic. 11 – Force - displacement plot for 1.2ASN

The result of a practical deep drawing operation is shown in picture n°12, the area where the break occurs correlates well to the failure predicted by the simulation.

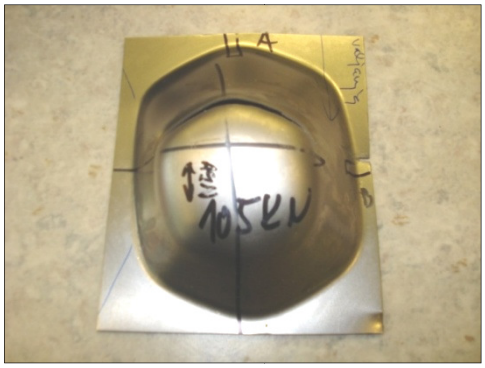

Pic. 12 – Deep drawing test on 1.2 ASN

The simulation performed with the material properties for 1.5 AL alloy indicates a more uniform stress and strain distribution than the one for 1.2 ASN. During the deformation, the peak stresses move from the leading edge of the punch to the inner edge of the die. There is no excessive stretching of the blank that would indicate possible failure during deep drawing.

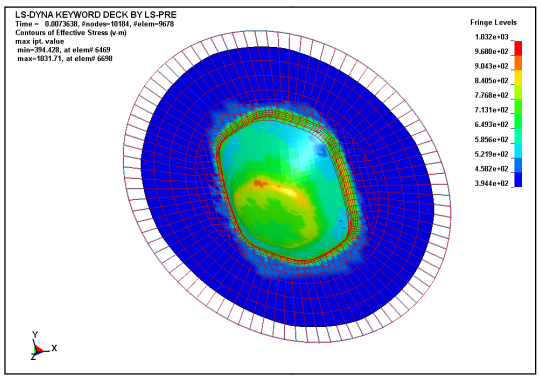

Pic. 13 – Von Misses effective stress for 1.5 AL

In this case the force-displacement plot does not show any irregularity; the deep drawing process can be completed without concerns.

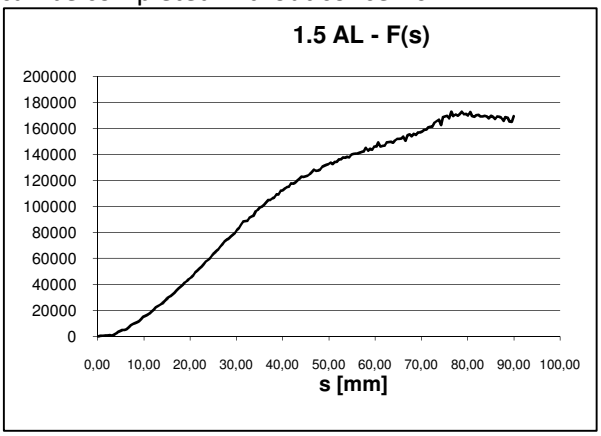

Pic. 14 – Force - displacement plot for 1.5 AL

6.2.2 FLD representation

For both considered alloys, the strains at the end of the forming process were plotted against the FLDs in the mayor-minor strain plot.

Picture n°15 clearly shows the localized deformation that exceeds the forming limit curve. Those points coincide with the excessive deformation at the leading edge of the punch.

Also note that in comparison to 1.2 ASN, the strains for 1.5 AL (picture n°16) are much more condensed on the FLD, providing a sufficient safety margin.

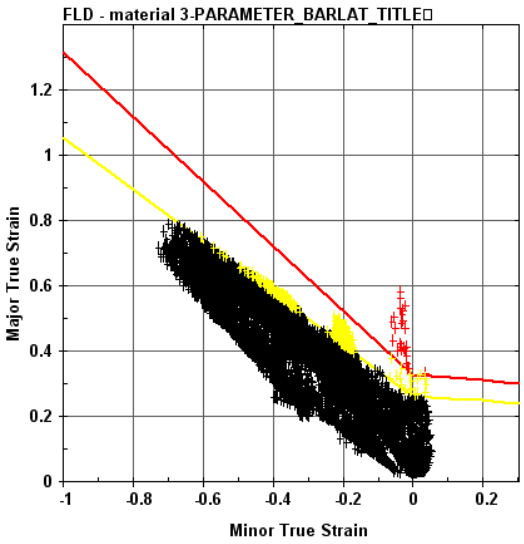

Pic. 15 – Strains displacement for 1.2 ASN

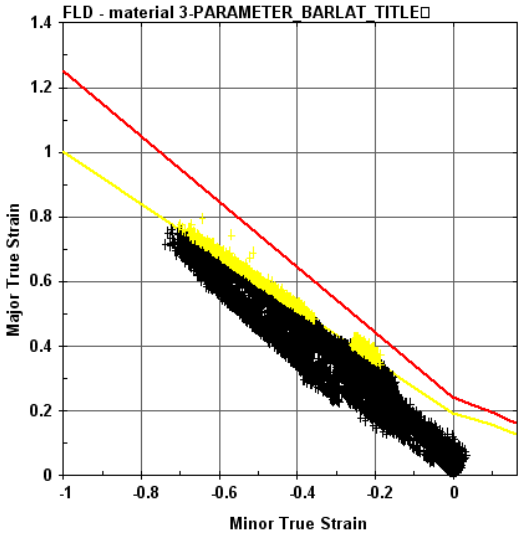

Pic. 16 – Strains displacement for 1.2 ASN

6.2.3 Thickness distribution

The simulated thickness distribution along the line shown in picture n°17 at the drawing depth of 47 mm was compared to the experimental thickness distribution measured on a real Q9 rosette drawn to the same depth. The 0 point on the horizontal axis corresponds to the die shoulder, with the distance measured along the surface of the rosette.

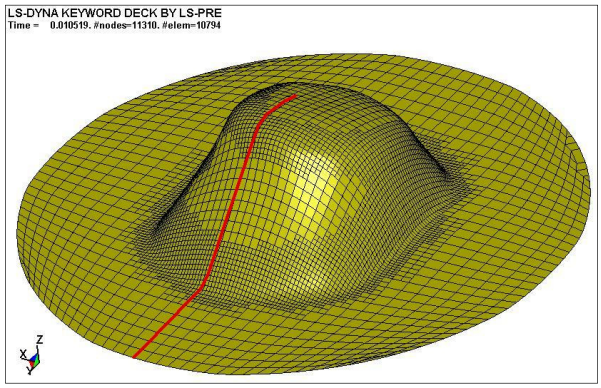

Pic. 17 – Thickness distribution line

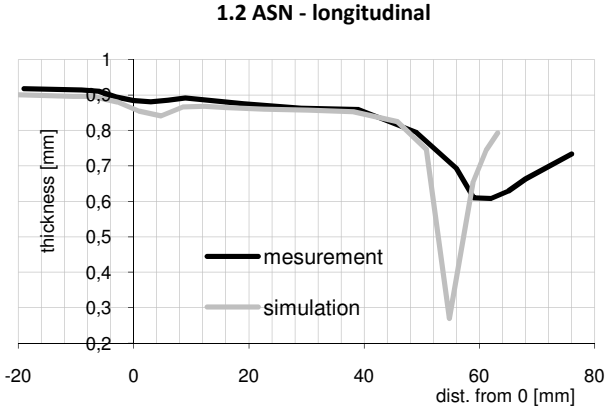

Pic. 18 – Thickness distribution in longitudinal dir. 1.2 ASN

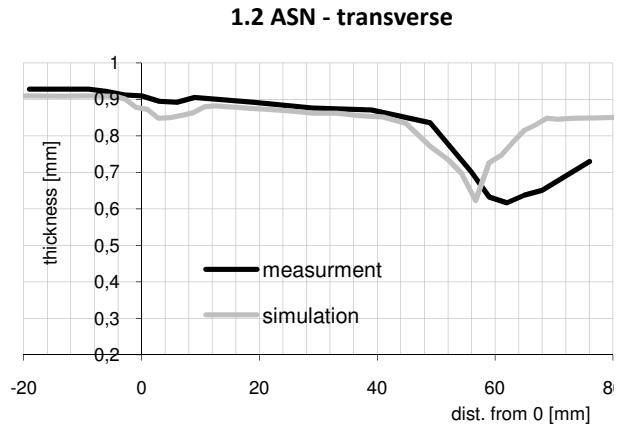

Pic. 19 - Thickness distribution in transverse dir. 1.2 ASN

As shown in Pic. *18* and *19*, the simulation results compare fairly well to the measurements; the severe discrepancy in the longitudinal direction is due to the simulation predicting a break in the rosette before this depth is achieved, which in itself tells us that the simulation is conservative.

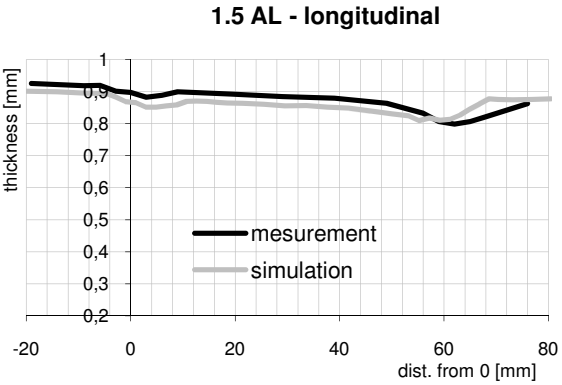

Pic. 20 - Thickness distribution in longitudinal dir. 1.5 AL

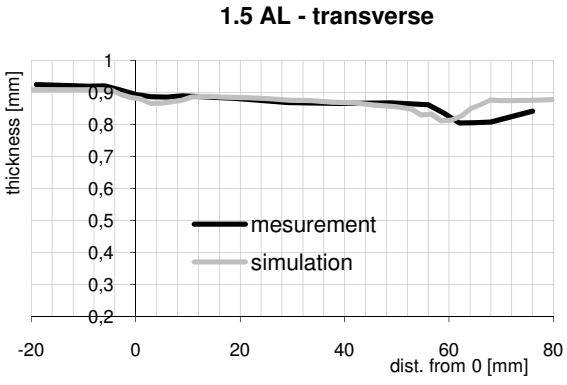

Pic. 21 - Thickness distribution in transverse dir. 1.5 AL

The diagrams represented in Pic. *20, 21* clearly show that 1.5 AL exhibits considerably less thinning in the critical region than 1.2 ASN. Although the thickness distribution does vary with blank orientation, longitudinal orientation giving a smoother transition into thinning and thus a more uniform thickness distribution than transverse, the minimal thickness in the critical region is quite similar.

7.0 CONCLUSIONS

The anisotropy of material has a fundamental role in deep drawing processes of α-Ti alloys. Experience acquired from working with Kobe Steel alloys 1.5 AL and 1.2 ASN has shown that when dealing with highly anisotropic materials judging their formability can be difficult and even counter-intuitive. None of the directly measurable material properties, such as hardening exponents and Lankford values, accurately describe the properties of these two materials relative one to the other, even the FLDs indicate that superior formability should be expected from 1.2 ASN (picture n°22), when practice clearly shows otherwise. The true behavior of these materials becomes obvious only when all these properties are input into a suitable FEM analysis, which clearly illustrates how both materials deform quite differently under the same conditions (Section 6.2.2).

The biggest influences on the strain distribution by far are the Lankford coefficients, which define the yield locus and thus the material flow, which is the defining factor in deep drawing. The hardening properties, although significant, play a secondary role.

The Barlat [1989] material model provided good results and proved to be quite adequate for deep drawing simulation of α-Ti alloys in an industrial environment, despite its lack of advanced emulation of phenomena associated with HCP materials.

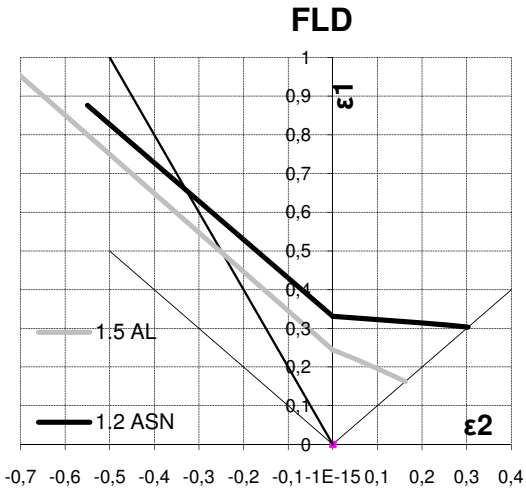

Pic. 22 – Comparison between FLDs diagrams

8.0 REFERENCES

[1] G. Lutjering, J.C. Williams – Titanium – Springer, second edition, p. 16

[2] G. Lutjering, J.C. Williams – Titanium – Springer, second edition, p. 20

[3] M. Hatherley, W.B. Hutchinson – An introduction to textures in metals pp.32-33 – Ed. Institution of metallurgists

[4] T.L. Sullivan, Texture strengthening and fracture toughness of titanium alloy sheet at room and cryogenic temperature – N.A.S.A. Technical Note D-4444

[5] M. Hatherley, W.B. Hutchinson – An introduction to textures in metals pp.57-58 – Ed. Institution of metallurgists

[6] LS-Dyna Keyword Users Manual Volume 2 V971-R4, LSTC, 2009.

[7] Cazacu O., Plunkett B., Barlat F. Orthotropic yield criterion for hexagonal close packed metals, International Journal of Plasticity, 2006 (22), p. 1171-1194.

[8] Lee M.G., Wagoner R.H., Lee J.K., Chung K., Kim H.Y. Constitutive modeling for anisotropic/asymmetric hardening behavior of magnesium alloy sheets, International Journal of Plasticity, 2008 (24), p. 545-582.

[9] Koc P., Štok B. Usage of the yield curve in numerical simulations, Journal of Mechanical Engineering, 2008 (54), p. 821-829.

9.0 CONTACTS

Dr. Eng. Silvia Gaiani
Akrapovič d.d.
Malo Hudo 8 – Ivancna Gorica (SLO)
silvia.gaiani@akrapovic.si

Sebastijan Jurendić B. Sc.
Akrapovič d.d.
Malo Hudo 8 – Ivancna Gorica (SLO)
sebatijan.jurendic@akrapovic.si

Prof. Paolo Veronesi
Materials Eng. Dept. – Modena University
Via Vignolese 905/A - Modena (I)
paolov@unimore.it

PURE POWER.

AKRAPOVIČ

PLASTIC DEFORMATION OF αTITANIUM ALLOYS SHEETS

Dr. Eng. Silvia Gaiani – Technical Director

TITANIUM 2010
Orlando, Florida
October 3-6th 2010

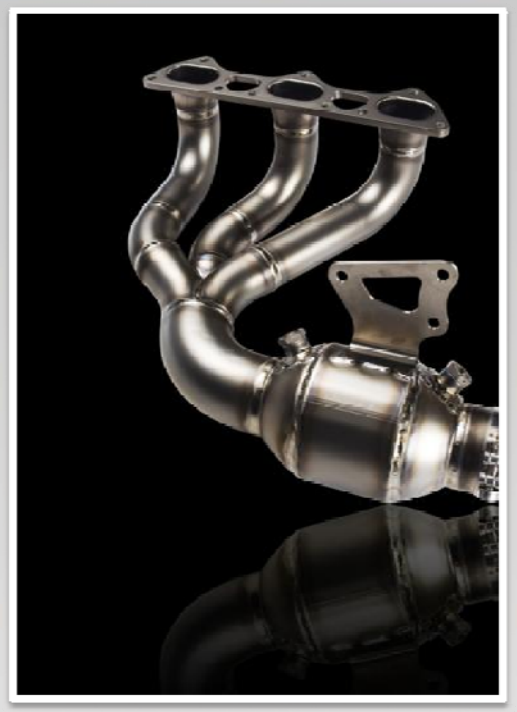

Titanium alloys used for exhaust system fabrication are currently all α alloys, which use small quantities of different alloying elements, as:

- **Aluminum**
- **Copper**
- **Niobium**
- **Silicon**
- **Iron**

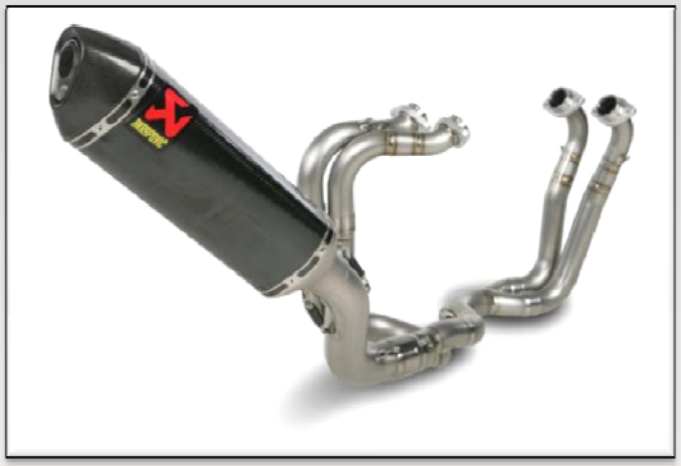

TITANIUM 2010
Orlando, Florida
October 3-6th 2010

These advanced alloys show excellent properties for their target application:

- Good strength
- Low density
- Oxidation resistance @ high T
- Weldability

However, their use for realizing parts with complicated shapes is still limited, because of problems associated with POOR FORMABILITY and consequently with high manufacturing costs

TITANIUM 2010
Orlando, Florida
October 3-6th 2010

Formability problems of α-Ti alloys are related to its type of lattice, which is Hexagonal Close Packed (HCP)

HCP lattice shows the following characteristics:

- Properties are related to the ratio between the height and width of the lattice (c/a ratio for Titanium is 1,587)

- Depending on c/a ratio, only 4 independent slip system are active, and they are not enough to allow plastic deformation (minimum 5)

- To allow plastic deformation, a system with a non-basal Burger vector needs to be activated. The activation of this slip system is tightly related to the direction of the load

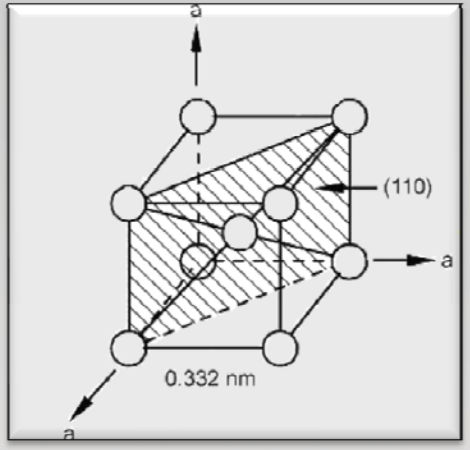

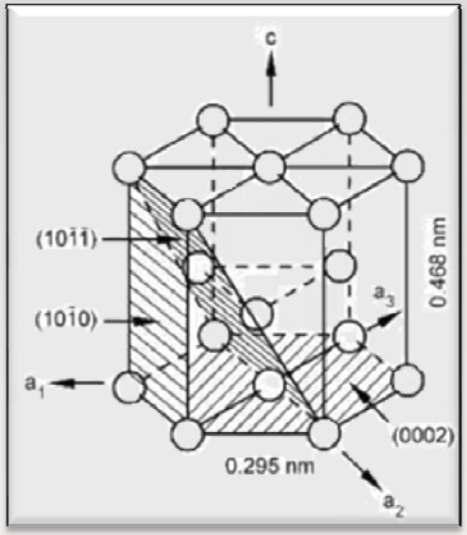

If stress axis // to c axis → NO ACTIVATION

TITANIUM 2010
Orlando, Florida
October 3-6th 2010

TWINNING occurs when two separate crystals share a part of the same lattice in a symmetrical manner. Deformation twinning is important for plasticity of HCP metals. In some conditions, depending on the stress direction and temperature, it can be predominant to dislocation slipping

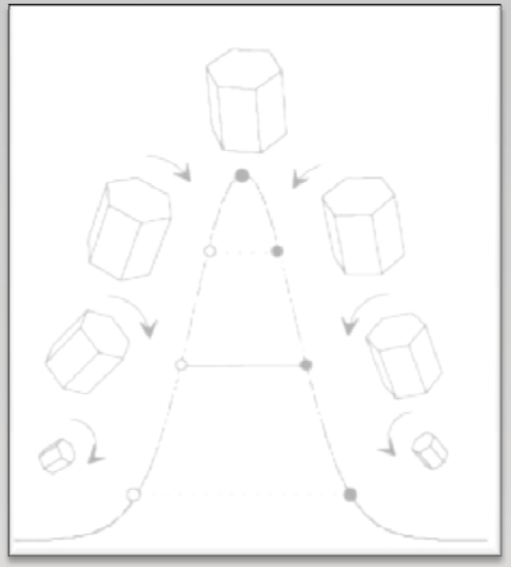

TEXTURING is a preferred orientation of the crystallographic structure. Texture is mainly determined by cold rolling conditions, heat treatments, alloying elements

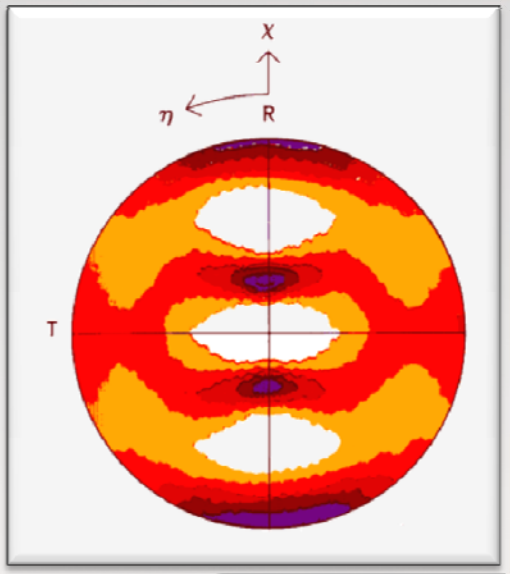

Because of the reasons mentioned above, Titanium α alloys exhibit <u>STRONG ANISOTROPIC BEHAVIOR</u>

TITANIUM 2010
Orlando, Florida
October 3-6th 2010

ANISOTROPY OF α-Ti

Moving from LONGITUDINAL direction to TRANSVERSE direction the properties are modified as follow:

- **Yield point increases**
- **Ultimate stress decreases**
- **Total elongation is equal**
- **Elongation at UTS is strongly reduced**

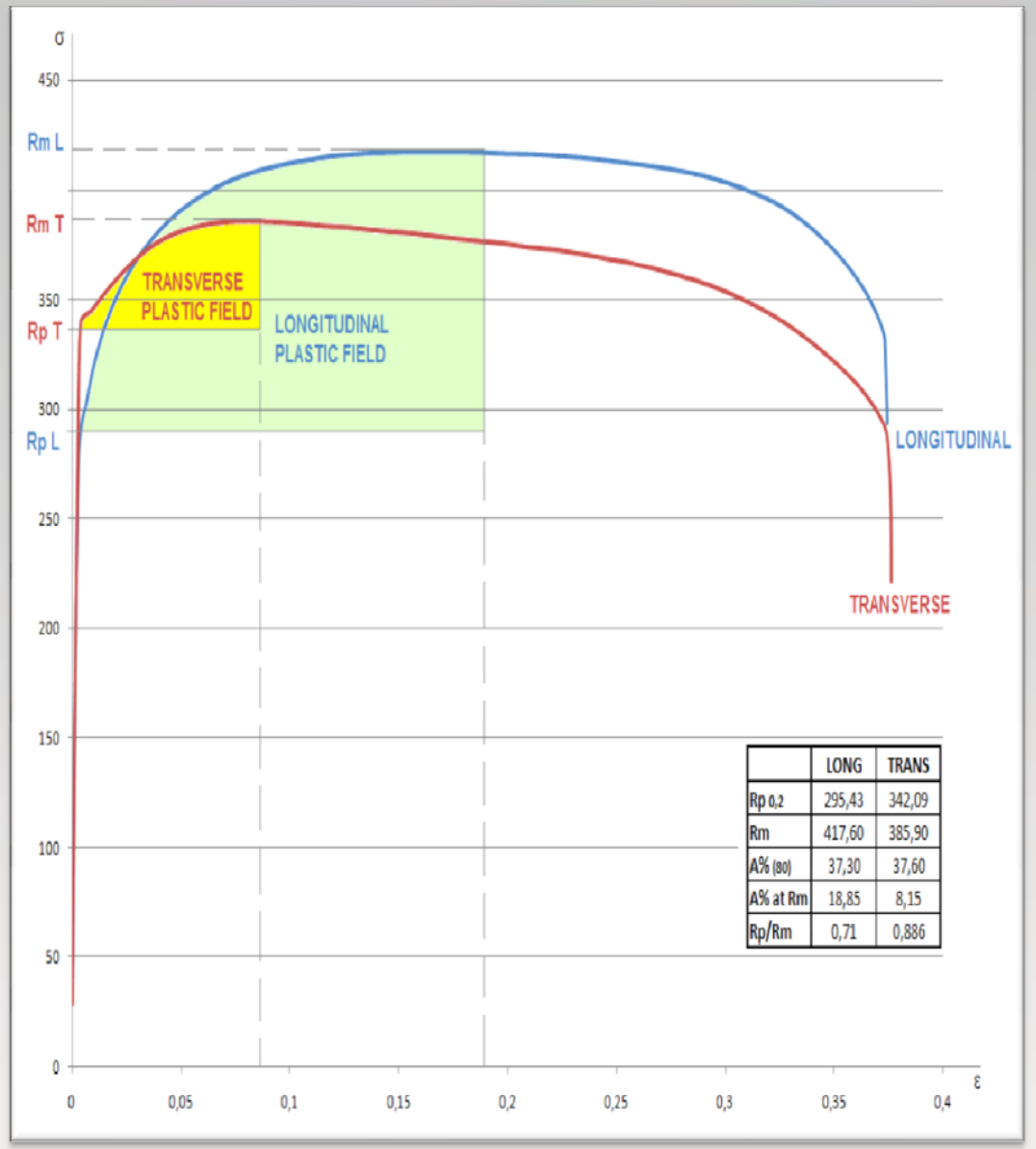

	LONG	TRANS
Rp 0,2	295,43	342,09
Rm	417,60	385,90
A% (80)	37,30	37,60
A% at Rm	18,85	8,15
Rp/Rm	0,71	0,886

TITANIUM 2010
Orlando, Florida
October 3-6th 2010

ANISOTROPY DETERMINATION

Plastic Strain Ratio: $r = \frac{\varepsilon_w}{\varepsilon_t}$

Normal anisotropy: $\bar{r} = \frac{r0^\circ + 2r45^\circ + r90^\circ}{4}$

Planar anisotropy: $\Delta r = \frac{r0^\circ - 2r45^\circ + r90^\circ}{2}$

The strain values ε_w and ε_t can be obtained performing a tensile test with a bi-axial strain gauge

Both normal and planar anisotropy are extremely important for predicting drawability, because they depend on plastic flow processes which take place in different areas of the metal

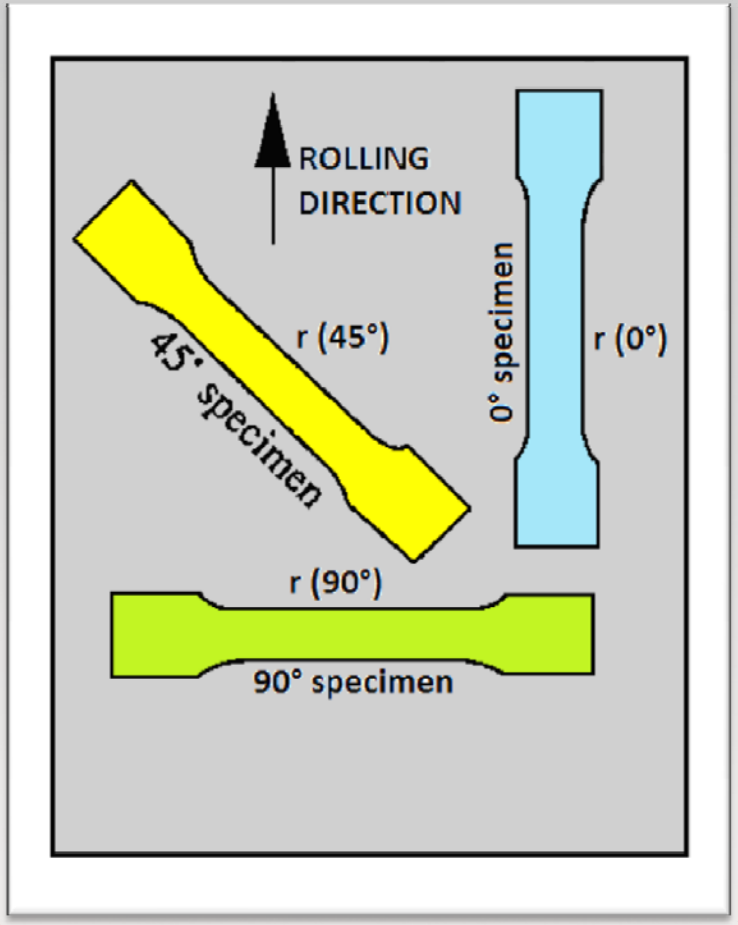

TITANIUM 2010
Orlando, Florida
October 3-6th 2010

DIFFERENT Ti-α ALLOYS COMPARISON

Two different types of alloys taken from our current production were investigated:

- KS 1,5 AL (Grade 37 ASTM B265)

- KS 1,2 ASN (patented alloy)

Both the materials are produced by the Japanese manufacturer Kobe Steel. 1,2 ASN alloy represents an improved version of Grade 37, especially in terms of oxidation resistance.

TITANIUM 2010
Orlando, Florida
October 3-6th 2010

EXPERIMENTAL DATA COLLECTION

Very similar mechanical characteristics:
1,2 ASN ~ 10% higher YTS and UTS, A% comparable

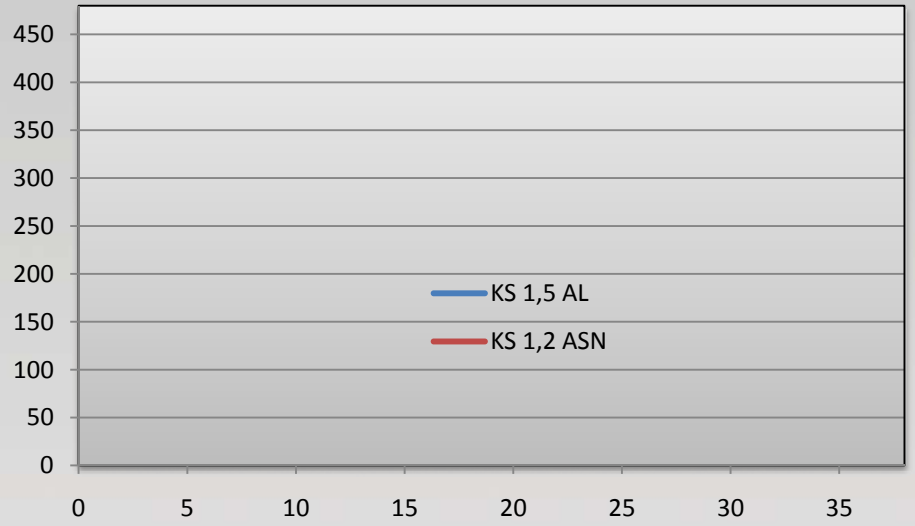

Lankford values in 0°, 90° and 45° vary less for 1,2 ASN – Normal anisotropy higher for 1,5 AL

Mat.	$R_{0°}$	$R_{90°}$	$R_{45°}$	$\bar{R}$	ΔR
1,2 ASN	1,6	4,3	2,7	2,825	0,25
1,5 AL	2,8	7,4	4,3	5,600	0,80

Strain hardening coefficients: comparable

Mat.	$n_{0°}$	$K_{0°}$ (MPa)	$n_{90°}$	$K_{90°}$ (MPa)	$n_{45°}$	$K_{45°}$ (MPa)
1,2ASN	0,154	710	0,086	590	0,112	596
1,5 AL	0,137	668	0,087	563	0,108	569

TITANIUM 2010
Orlando, Florida
October 3-6th 2010

MODELLING OF PLASTIC RESPONSE

For the simulation of anisotropic behavior of α-Ti alloys sheets, the Barlat 1989 plane stress criterion has been chosen:

$$\Phi = a\left|K_1 + K_2\right|^m + a\left|K_1 - K_2\right|^m + c\left|2K_2\right|^m = 2\sigma_Y{}^m$$

Where:

$$K_1 = \frac{\sigma_x + h\sigma_y}{2} \qquad K_2 = \sqrt{\left(\frac{\sigma_x - h\sigma_y}{2}\right)^2 + p^2\tau_{xy}{}^2}$$

- σ_x and σ_y are stresses in rolling and transverse direction
- a, c, h, p are material parameters which are directly related to strain ratio values R
- m is the flow potential exponent (defines the shape of the yield curve); is related to the type of crystal lattice

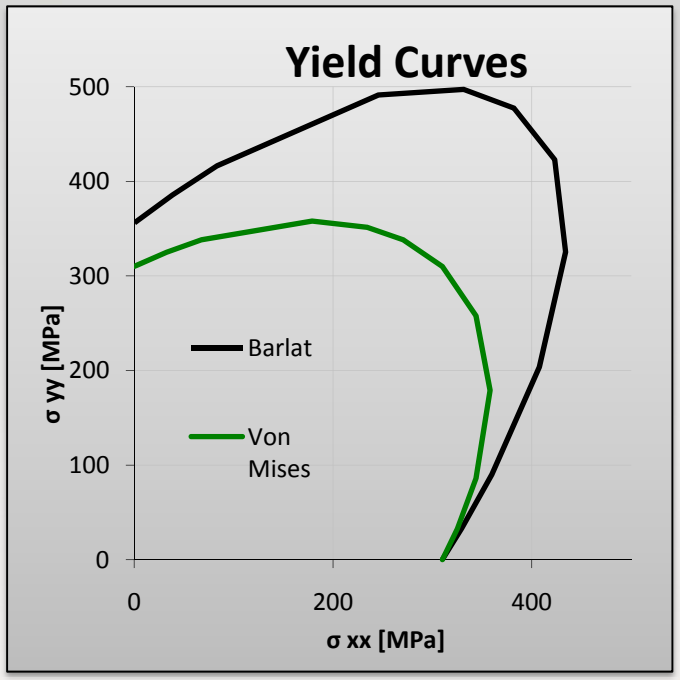

TITANIUM 2010
Orlando, Florida
October 3-6th 2010

INPUT DATA FOR FEA MODELLING

1) Lankford coefficients in three directions R_{00}, R_{45}, R_{90}: they are derived directly from the tensile test with the bi-axial strain gauge

2)Yield stress function $\sigma_Y\left(\bar{\varepsilon}_p\right)$ in rolling direction
This function can be defined in two different ways:

- Inserting the n and K parameters obtained from the tensile test directly into the Hollomon equation
- Using an experimental curve obtained by simulating the uniaxial tensile test

3) Flow potential exponent m
The exponent can be obtained in two different ways:

- Using data collected from literature (very rare)
- Deducing the correct value by simulating the Erichsen test

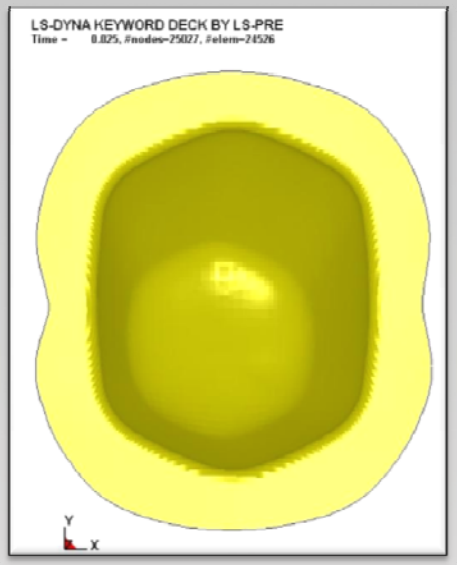

TITANIUM 2010
Orlando, Florida
October 3-6th 2010

TRUE σ – TRUE ε CURVE DETERMINATION

1st Attempt: using the Hollomon equation $\sigma = K\varepsilon^n$ with strain hardening values obtained from the tensile test

Results: fit of the curve at higher strains very poor

2nd Attempt: using an inverse procedure where numerical simulations of the tensile test are used to iteratively modify the load curve until the calculated response matches the data from the tensile test

Results: very positive

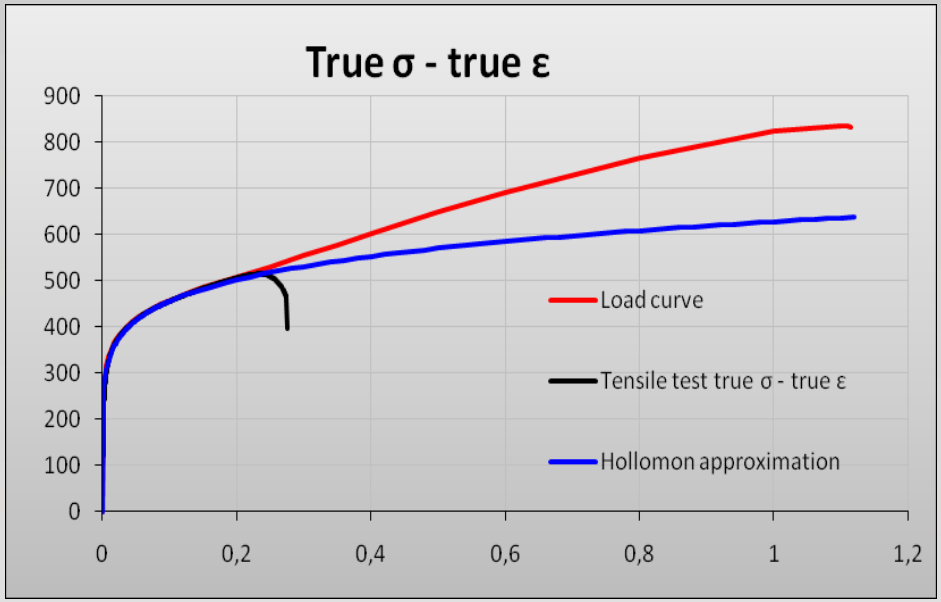

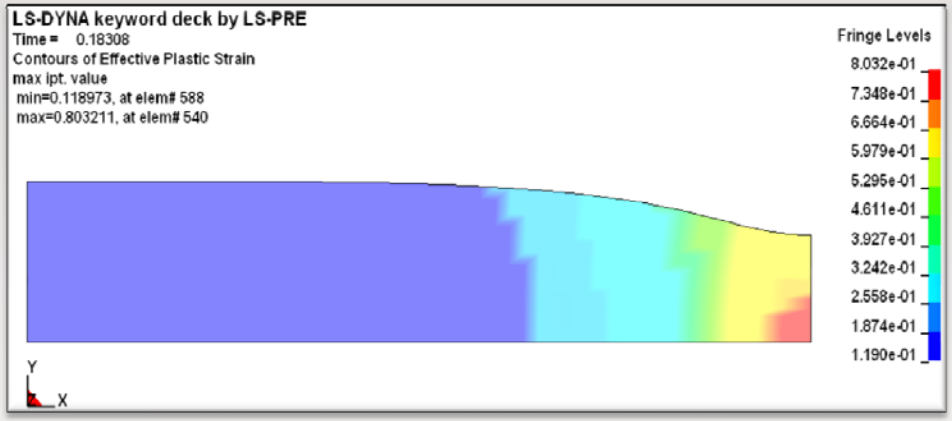

TITANIUM 2010
Orlando, Florida
October 3-6th 2010

m PARAMETER DETERMINATION

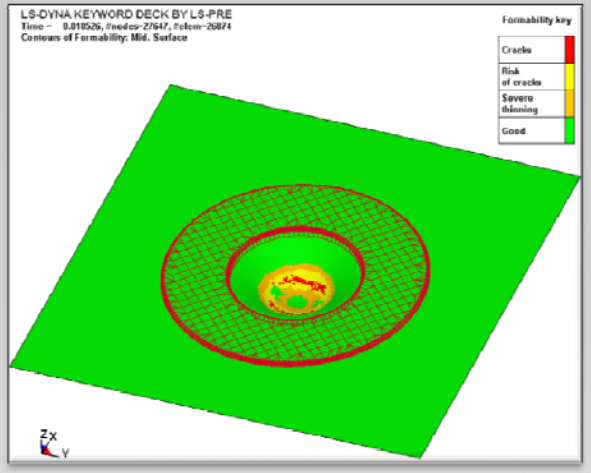

1st Attempt: using existing data found in literature

Results: no reliable data was found for this particular type of crystal lattice

2nd Attempt: using an inverse procedure, in this case simulating the Erichsen test; numerical trials were run for a range of different *m* parameters and the results compared to the experimental data

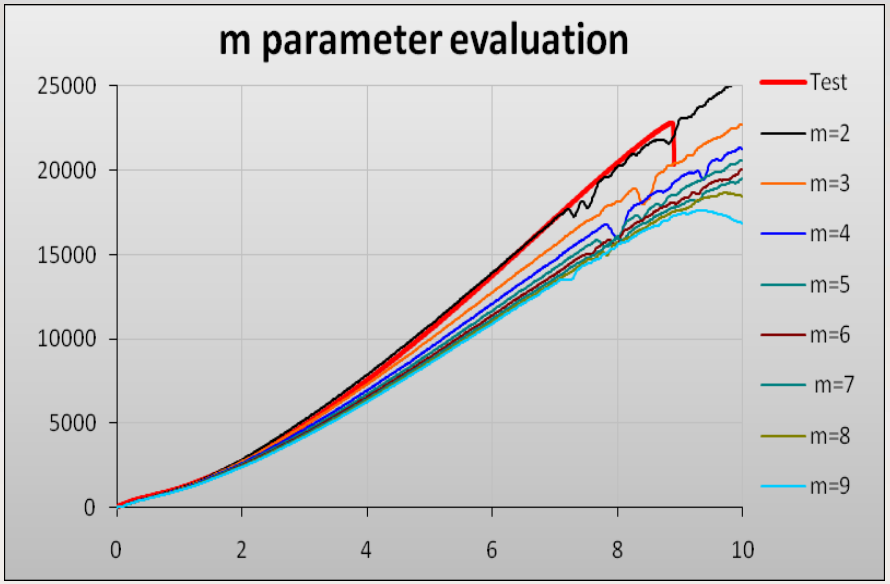

Results: positive but not perfect
(many parameters effect the real test)

DEFORMATION LIMITS: FLD DIAGRAM

For determination of the upper limit of formability, a knowledge about FLD diagrams is required.
In order to obtain the FLDs, a series of compressive tests using a hemi-spherical punch have been carried out using the Aramis optical 3D forming analysis system for strain measurement.

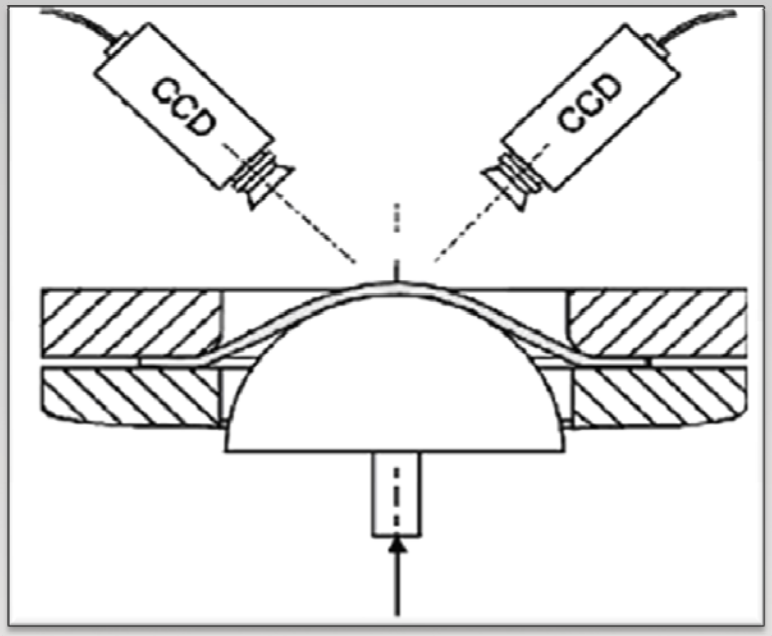

The Nakajima test method has been chosen; for every single alloy seven geometries have been tested for a total of 42 tests

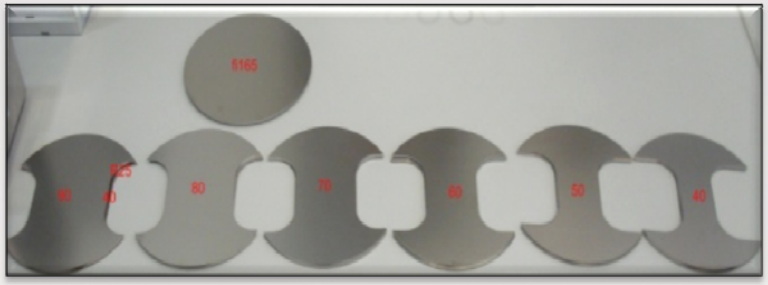

TITANIUM 2010
Orlando, Florida
October 3-6th 2010

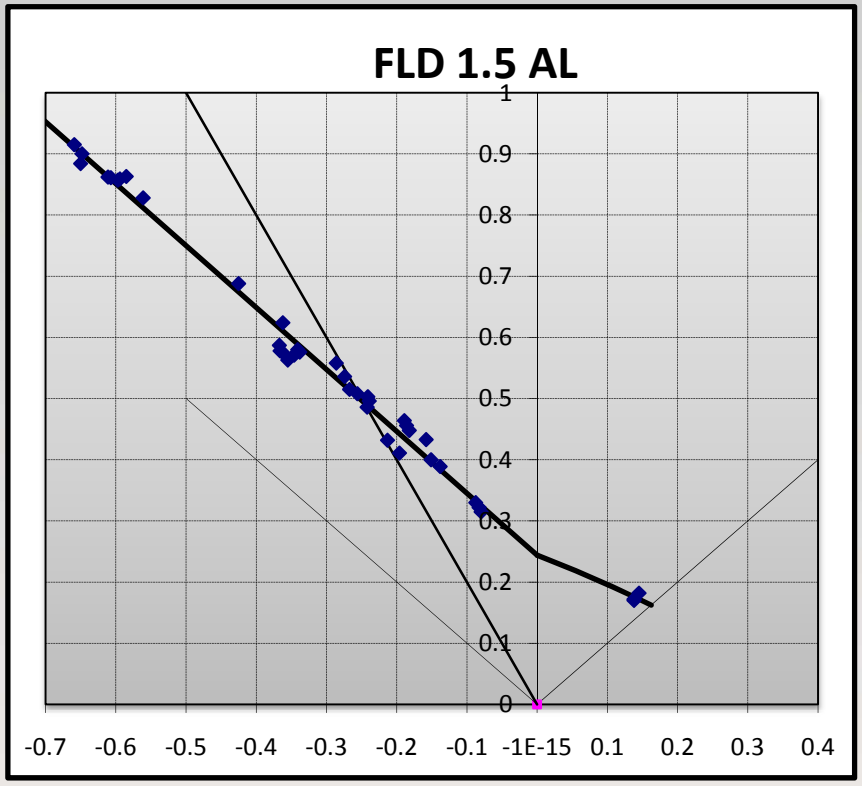

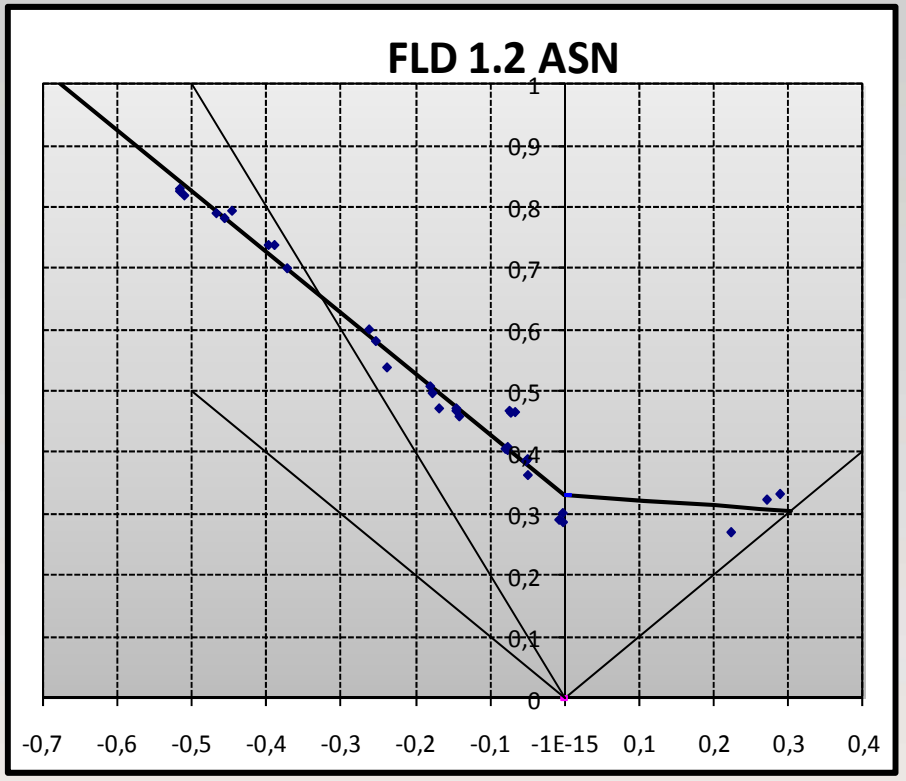

TITANIUM 2010
Orlando, Florida
October 3-6th 2010

NUMERICAL SIMULATION OF Q9 ROSETTE

SIMULATION CONDITIONS

Blank: 2D shell elements, Belytschko - Tsay formulation, 5 Gauss integration points

Tools: idealized rigid 2D shell

Blank orientation: rolling direction parallel and perpendicular to the length of the rosette

Punch Movement: constant speed up to 90mm and than retracted (for spring back analysis)

Blank holder: constant force of 100kN (~10 metric tons)

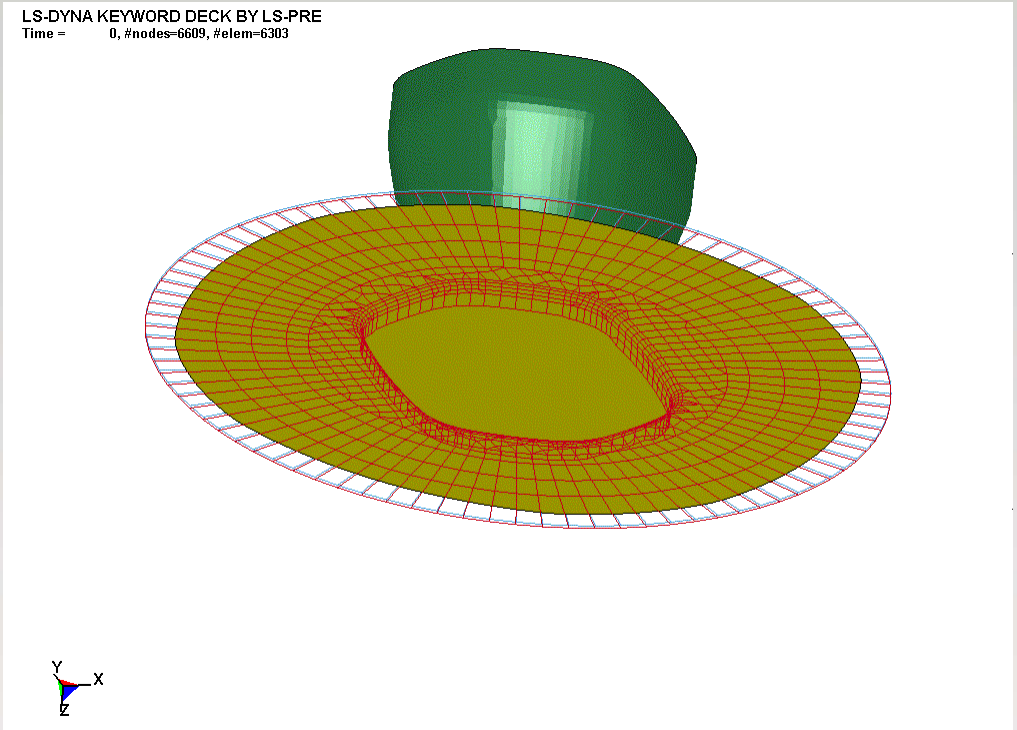

TITANIUM 2010
Orlando, Florida
October 3-6th 2010

STRESS DISTRIBUTION & FORCE DISPLACEMENT

1,2 ASN

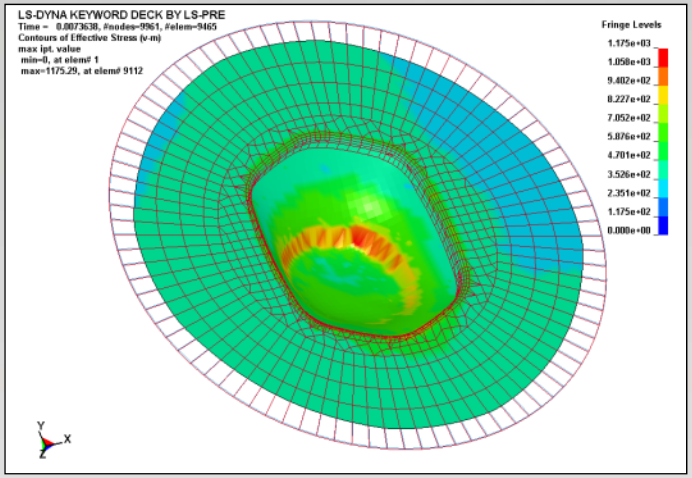

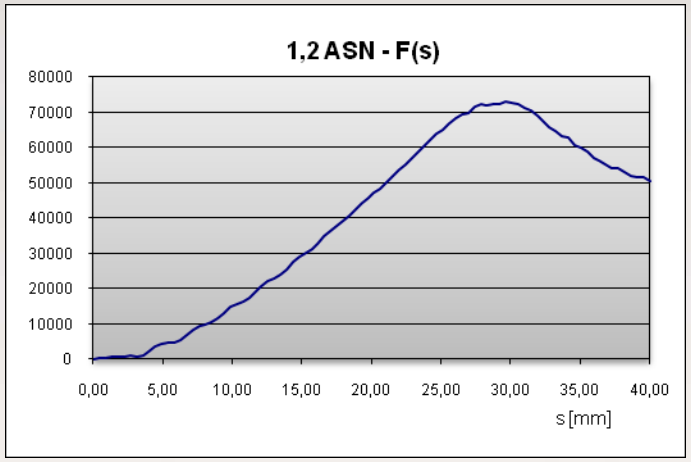

1,5 AL

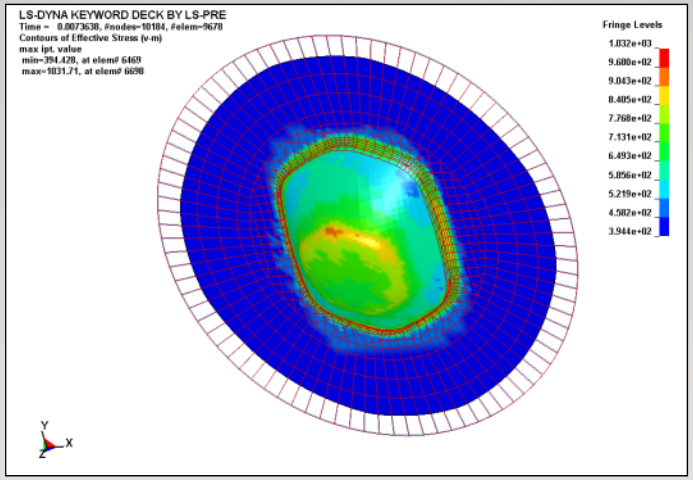

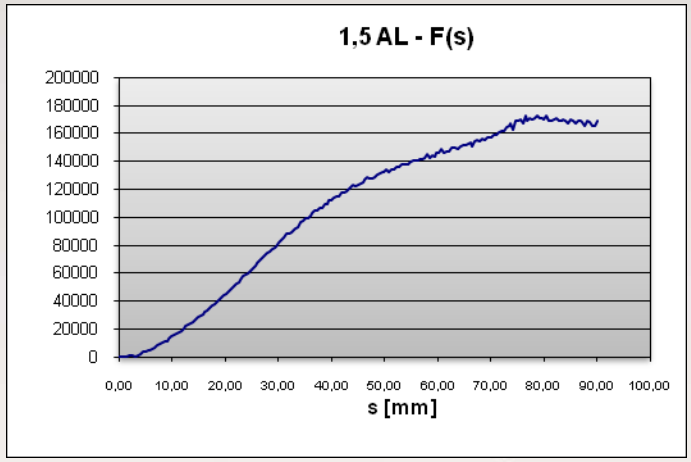

TITANIUM 2010
Orlando, Florida
October 3-6th 2010

1,2 ASN

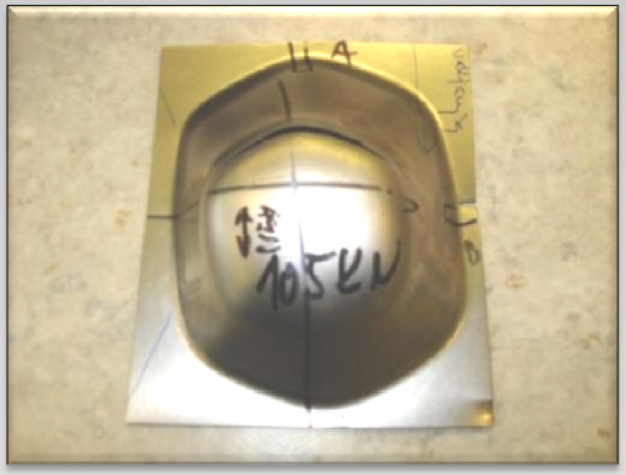

Simulation using 1,2 ASN alloy shows strong stress localization around the leading edge of the punch, at around 30mm of displacement there is excessive stretching of the blank indicating material failure

1,5 AL

The simulation performed with 1,5 AL alloy indicates a more uniform stress and strain distribution. During deformation the peak stresses are relocated to the inner edge of the die. There is no excessive stretching that would indicate possible failure during deep drawing

TITANIUM 2010
Orlando, Florida
October 3-6th 2010

DEFORMATION ON FLD DIAGRAM

1,2 ASN

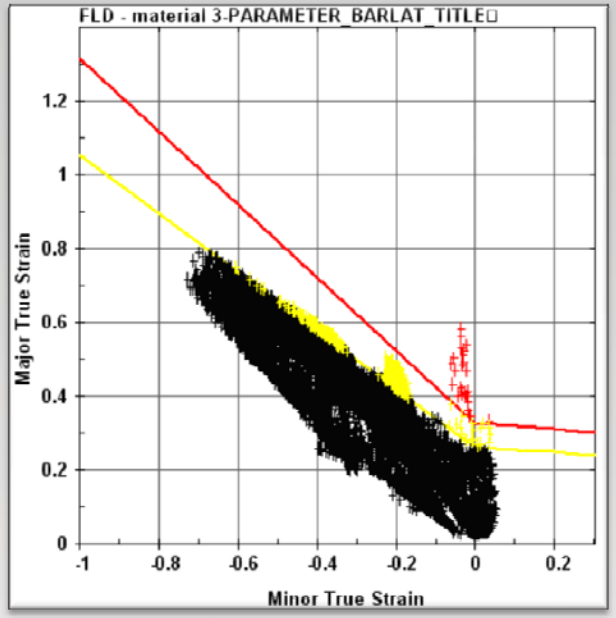

For 1,2 ASN, the excessive localized deformation at the leading edge of the punch is obvious on the forming limit curve

1,5 AL

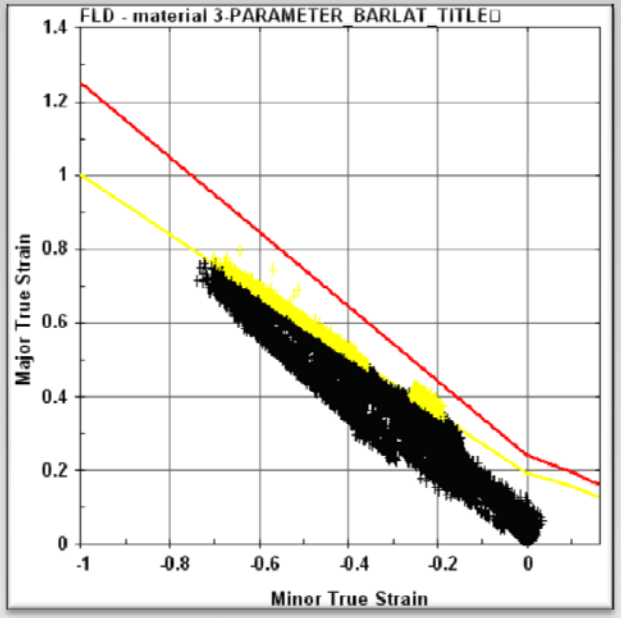

The strains for 1,5 AL are much more condensed on the FLD, providing a sufficient safety margin

TITANIUM 2010
Orlando, Florida
October 3-6th 2010

THICKNESS DISTRIBUTION

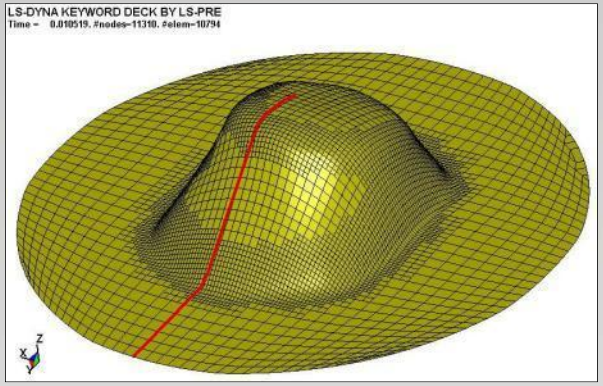

A thickness measurement has been performed along the marked section, using an ultrasonic device. The results were then compared with the simulations. The 0 point on the abscissa corresponds to the die shoulder

1,2 ASN

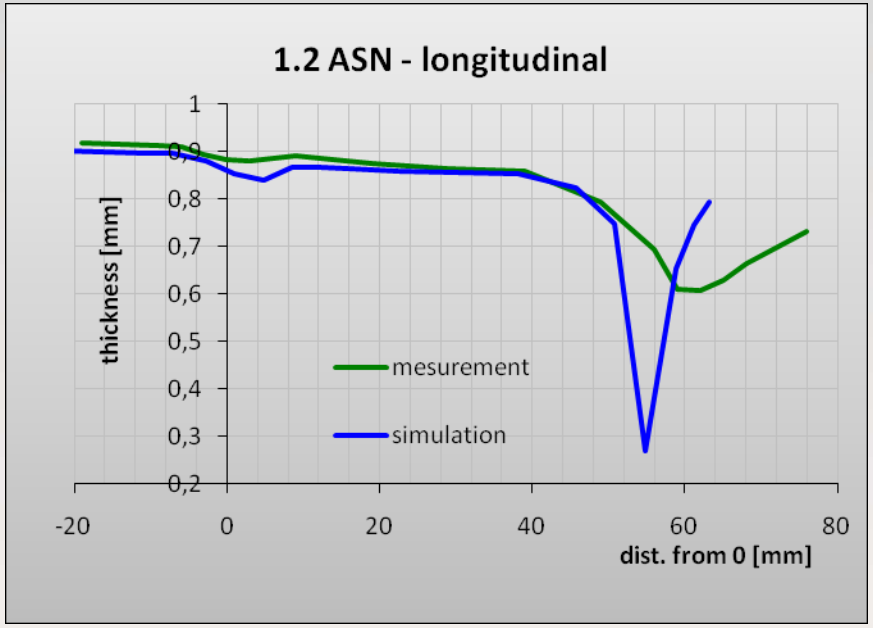

1,5 AL

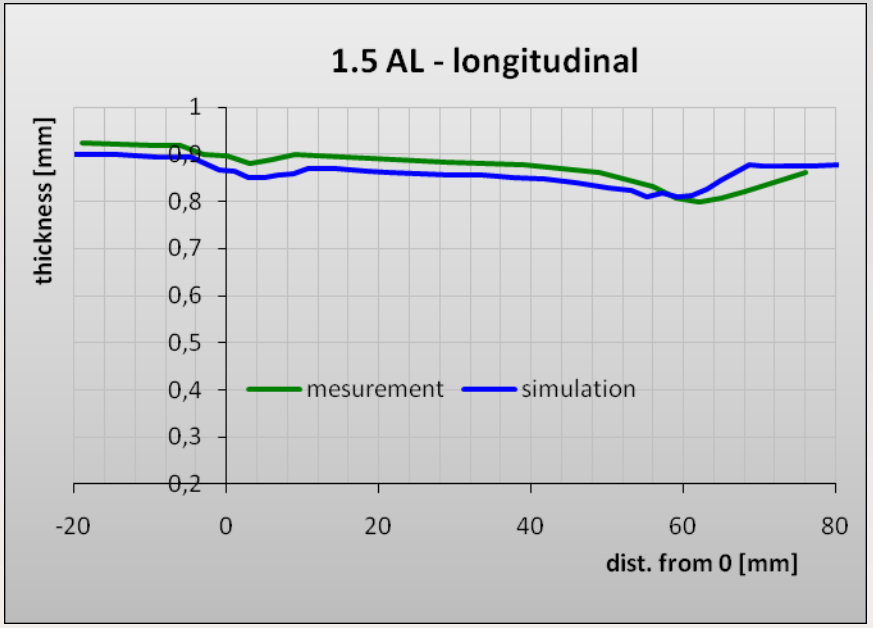

TITANIUM 2010
Orlando, Florida
October 3-6th 2010

1,2 ASN

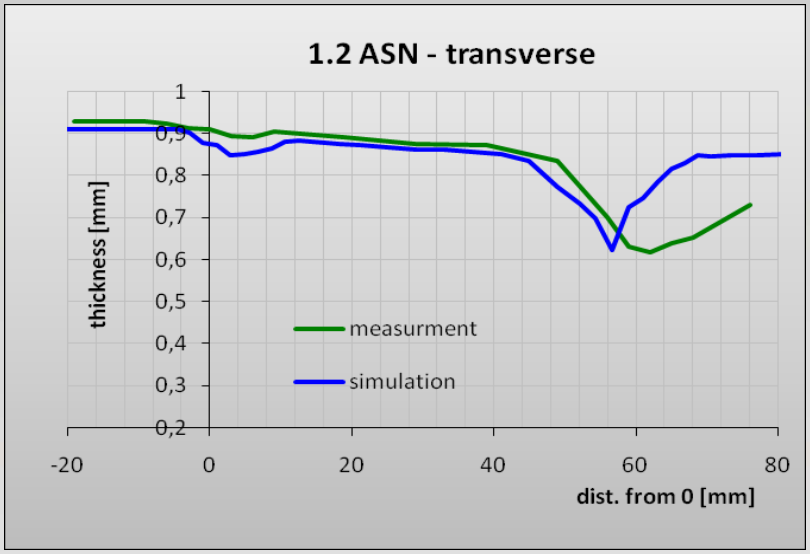

The simulation results compare fairly well to the measurements; the discrepancy in the longitudinal direction is due to the simulation predicting a break in the rosette before this depth is achieved. This shows that the simulation is conservative

1,5 AL

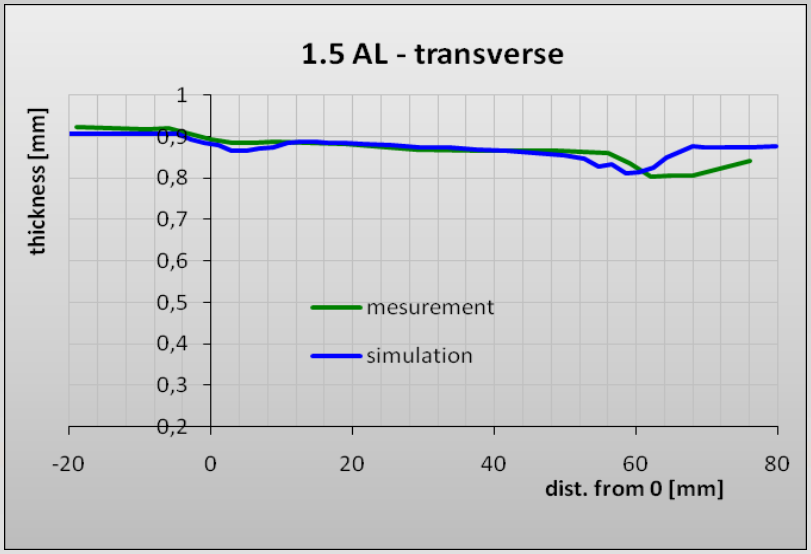

The diagrams clearly show that 1,5 AL exhibits considerably less thinning in the critical region than 1,2 ASN

TITANIUM 2010
Orlando, Florida
October 3-6th 2010

CONCLUSIONS

- Experience acquired working with Kobe Steel alloys 1,5 AL and 1,2 ASN has shown that when dealing with highly anisotropic materials judging their formability can be difficult and even counter-intuitive

- None of the directly measurable material properties, such as hardening exponents n, K and Lankford values R, Erichsen index or even the FLD diagrams accurately describe the properties of these two materials relative one to the other

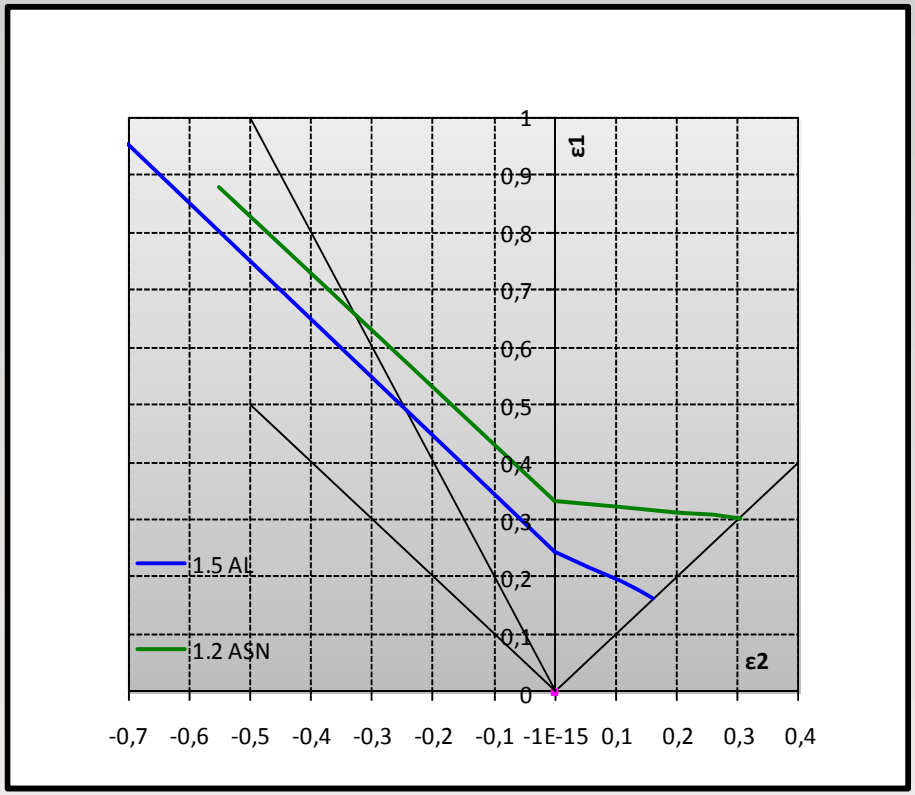

TITANIUM 2010
Orlando, Florida
October 3-6th 2010

- The Barlat [1989] material model, implemented with experimental parameters, provided good results in simulating deep drawing of α-Ti alloys
- Numerical modeling is the best instrument for illustrating how different alloys deform under the same loading conditions and how different strain distributions are produced
- Currently we are working on implementing strain rate sensitivity effects into the numerical model